Biotechnol Lett (2016) 38:259–269
DOI 10.1007/s10529-015-1981-3

ORIGINAL RESEARCH PAPER

PLA nanovectors with encapsulated betulin: plant leaf extract-synthesized nanovectors are more efficacious than PVA-synthesized nanovectors

Ramdhan Yadav · Dharmesh Kumar · Avnesh Kumari · Sudesh Kumar Yadav

Received: 9 September 2015 / Accepted: 12 October 2015 / Published online: 17 October 2015

Abstract
Objectives Betulin (BT) is an abundant triterpene found predominantly in the bark of Himalayan birch. It is difficult to deliver it in vivo because of its low aqueous solubility. We have therefore developed novel formulations of BT for improving its solubility, bioavailability and therapeutic efficacy.
Results Poly-D,L-lactide nanovectors (PLA NVs) were synthesized using poly(vinyl alcohol) and *Lonicera japonica* leaf extract (LE) as a stabiliser and named as PLA-1 NVs and PLA-2 NVs. PLA-1 NVs and PLA-2 NVs were used for the encapsulation of betulin (BT) and named as BT-En-1 and BT-En-2 NVs. The encapsulation efficiency of BT-En-1 and BT-En-2 NVs were 99.3 and 100 % respectively. Prepared nanoformulations were physically stable. An in vitro study revealed 45 % BT was released over 24 h. BT had a prolonged release from BT-En-2 NVs as compared to BT-En-1 NVs. BT-En-2 NVs had better anticancerous activity against SiHa cells than BT-En-1 NVs.
Conclusions Developed BT-EN-2 NVs had better biocompatibility, excellent stability and enhanced release characteristics than BT-En-1 NVs.

Keywords Anticancer activity · Betulin · Encapsulation · Leaf extract · *Lonicera japonica* · Nanovectors · Poly-D,L-lactide

Introduction

Betulin (BT) is a highly effective anticancer agent. However, its clinical applications are limited due to its poor aqueous solubility and low bio-accessibility (Jager et al. 2008; Gauthier et al. 2009). Towards this effort, BT had been derivatized or mixed with cholesterol to enhance therapeutic activity (Mullauer et al. 2009). BT with semisynthetic cyclodextrins has improved solubility and bioavailability but poor stability (Soica et al. 2012). BT has also been covalently conjugated with anionic polyelectrolytes and water-soluble bovine serum albumin to enhance its bioavailability (Mustafaev et al. 2002).

The field of nanomedicine seeks to improve pharmacokinetics of therapeutic cargos through design of nanovectors (NVs). Encapsulation of different bioactive molecules in NVs protects them from degradation, increases their half lives and reduces their toxicity. NVs also improve the release characteristics

Electronic supplementary material The online version of this article (doi:10.1007/s10529-015-1981-3) contains supplementary material, which is available to authorized users.

R. Yadav · D. Kumar · A. Kumari · S. K. Yadav (✉)
Biotechnology Division, CSIR-Institute of Himalayan Bioresource Technology, Council of Scientific and Industrial Research, Palampur, H. P. 176061, India
e-mail: sudeshkumar@ihbt.res.in; skyt@rediffmail.com

R. Yadav · S. K. Yadav
Academy of Scientific and Innovative Research, New Delhi, India

and enhance the therapeutic efficacy of bioactive molecules (Kumari et al. 2011; Yadav et al. 2011, 2014a, b). Among various NVs, poly-D,L-lactide (PLA) has attracted attention for a wide range of anticancer cargos. PLA NVs exhibit excellent biocompatibility and good encapsulation of hydrophobic anticancer agents. But PLA NVs synthesized using chemical stabilisers may be toxic. To reduce the toxicity of chemically-synthesized PLA NVs, various plant extracts have been explored. Extracts of many medicinally-important plants have shown good potential for the synthesis of PLA NVs (Kumari et al. 2012, 2014). Also the PLA NVs synthesized with plant-based stabilisers are biocompatible. Further, if the plants have medicinally important biomolecules, they may enhance the value of synthesized NVs. To enhance the therapeutic index of bioactive molecules, the synthesized NVs with bioactive molecules should be non-toxic and biocompatible. Therefore, evaluation of synthesized NVs for toxicity before their further use is required.

Hence, it is critical to develop novel nanovectors (NVs) to improve the therapeutic efficacy and reduce the side effects of BT. In view of this, we report for the first time the encapsulation of BT in PLA NVs. We have prepared two types of PLA NVs using polyvinylalcohol (PVA) and a leaf extract as stabiliser. These were used for BT encapsulation and named as BT-En-1 NVs and BT-En-2 NVs, respectively. They have been characterised using various technologies. The entrapment efficiency, drug loading and in vitro release of BT from BT-En-1 NVs and BT-En-2 NVs were quantified by HPLC. Additionally, the physical stability of BT-En-1 NVs and BT-En-2 NVs was analysed. The anticancer activity of loaded BT-En-1 NVs and BT-En-2 NVs and their respective blank NVs were also investigated against human cervical cancer (SiHa) cells.

Materials and methods

Materials

Betulin, poly-D,L-lactide (PLA; Mw = 75,000–120,000), and polyvinyl alcohol (PVA) were purchased from Sigma-Aldrich. Dichloromethane (DCM) was purchased from Merck. Solutions were prepared using milli-Q water (Millipore, Bedford, MA). Leaves of *Lonicera japonica* were obtained from the CSIR-IHBT campus. Human cervical cancer cells (SiHa) were obtained from NCCS (National Centre for Cell Science), Pune, India. Cells were cultured in RPMI-1640 (Invitrogen) supplemented with 10 % (v/v) heat-inactivated fetal bovine serum (Invitrogen) and 1 % (w/v) antimycotic antibiotic (Invitrogen). The cells were maintained at 37 °C in a 5 % CO_2 humidified atmosphere.

Leaf extracts

Dried leaves of *Lonicera japonica* were crushed to fine powder and 4 g were mixed with 50 ml milli-Q water, vortexed and stirred overnight. The suspension was centrifuged at $\sim 10{,}000 \times g$ and supernatant was filtered through a 0.2 um filter to obtain the leaf extract (LE).

Synthesis of PVA and LEs-mediated BT-loaded PLA NVs

LEs (leaf extracts) and PVA-mediated NVs were prepared by solvent evaporation. In PVA-mediated synthesis, 50 mg PLA and 5 mg betulin was dissolved in 2 ml DCM and sonicated for 40 s. The solution was mixed with freshly prepared 4 ml (3 % w/v) PVA and again sonicated to form an emulsion. This was diluted in 0.1 % (w/v) PVA to make 80 ml. DCM was evaporated under vacuum using rotating evaporator. The NVs were separated by centrifugation at $\sim 10{,}000 \times g$ for 15 min at 10 °C and obtained NVs were then washed twice with milli-Q water. PLA NVs alone were prepared by procedure as described above but without addition of BT. PLA NVs synthesized using PVA was named as PLA-1 NVs. PLA-1 NVs encapsulated with BT was named as BT-En-1 NVs.

Plant-mediated synthesis of PLA NVs was carried out using LEs of *Lonicera japonica* as stabiliser. Five mg BT and 50 mg PLA were dissolved in 2 ml DCM and sonicated for 50 s in pulsed mode at 40 % amplitude in ice. The above solution was mixed with 5 ml LEs and again sonicated for 50 s to form an emulsion. This was diluted by milli-Q water to make 80 ml. DCM was removed by rotating evaporator under vacuum at 40 °C. LEs-mediated BT- loaded NVs were separated by centrifugation at $\sim 10{,}000 \times g$, washed twice with milli-Q water and stored at 4 °C. PLA NVs alone were prepared by same procedure without addition of BT. PLA NVs synthesized using LEs was named as PLA-2 NVs. PLA-2 NVs encapsulated with BT was named as BT-En-2 NVs.

Spectroscopic characterisation of NVs

Reaction mixtures were evaluated for the synthesis of PLA NVs on Nanodrop ND-2000 with path length of 1 mm and 2048 element linear silicon CCD array detector.

The infrared spectra of solid BT-En-1 NVs, BT-En-2 NVs and pure BT were recorded with a Thermo Nicolet 6700 FTIR spectroscopy (Thermo, USA). The spectra were recorded on the KBr pellets in the scanning range of 400–4000 cm^{-1} at 2 cm^{-1} resolution.

Morphological characterisation of NVs

Morphology of PLA-1 NVs, PLA-2 NVs, BT-En-1 NVs and BT-En-2 NVs was characterised using the atomic force microscope (AFM) (Nanoscope-III, Veeco Instruments, Singapore). A drop of synthesized NVs were uniformly spread on the freshly-cleaved clean glass surface and dried at room temperature in dust-free conditions. Images were taken in the tapping mode using silicon probe cantilever of 125 μm length, resonance frequency of 209–286 kHz, spring constant of 20–80 N/m and nominal, 5–10 nm tip radius of curvature and scan rate of 1 Hz.

Transmission electron microscopy (FEI, Netherlands) was used for shape and size measurement of PLA-1, PLA-2, BT-En-1 and BT-En-2 NVs. The images were obtained with a Tecnai, Twin 200 kV TEM (FEI, Netherlands) operated at 200 kV at desired magnification.

Dynamic light scattering technique (DLS) was also used for size as well as zeta potential evaluation of all synthesized NVs. Water suspended each NVs were diluted four times and subjected to size and zeta potential measurements in disposable cuvettes on Zetasizer Nano ZS (Malvern).

Physical stability of NVs at physiological temperature

The stability analysis of PLA-1, PLA-2, BT-En-1 and BT-En-2 NVs was carried out in aqueous solution at 37 °C for 45 days. The DLS was used to measure the zeta potential on days 1, 5, 15, 30 and 45. Samples were also monitored after a regular interval and TEM analysis was performed after 45 days.

Encapsulation efficiency evaluations of BT in BT-En-1 NVs and BT-En-2 NVs

Encapsulation efficiency of BT on BT-En-1 NVs and BT-En-2 NVs was measured by HPLC. The supernatant (10 μl) of BT-En-1 and BT-En-2 NVs obtained after the separation of NVs by centrifugation was filtered through 0.22 μm filters. Supernatant was lyophilized, re-dissolved in methanol, centrifuged at $\sim 10{,}000 \times g$ for 20 min and analysed by HPLC having a reverse phase C18 column (150 mm × 4.6 mm, 5 μm). The mobile phase was acetonitrile/water (90:10, v/v) at 1 ml/min with detection at 210 nm. A calibration curve was generated using BT from 0.0625 to 1 mg/ml. The correlation coefficient was 0.999. The regression equation generated by calibration curve was $2 \times 10^6 X + 47851$ and it was used to calculate the amount of BT present in supernatant. The encapsulation efficiency and the BT loading (%) were calculated using equations given below:

$$EE\ (\%) = \left(\frac{amount\ of\ BT\ entrapped}{total\ amount\ of\ BT\ in\ formulation}\right) \times\ 100 \tag{1}$$

$$BT\ \ loading\ (\%)\ \ =\ \left(\frac{mass\ of\ BT\ entrapped\ in\ nanoparticles}{mass\ of\ nanoparticles\ recovered\ after\ lyophilisation}\right)\ \times\ 100. \tag{2}$$

In Vitro release assay of BT from BT-En-1 NVs and BT-En-2 NVs

The in vitro release kinetics of BT was performed by incubating 5 mg BT-En-1 NVs and BT-En-2 NVs individually in 10 ml 0.1 M phosphate buffer/saline (pH 7.4). The BT-En-1 NVs and BT-En-2 NVs were continuously stirred by a magnetic stirrer (120 rpm) at 37 °C. The released sample containing BT (1 ml) was collected at 0, 2, 4, 6, 8, 12, 16, 20, 24, 28 and 32 h, lyophilized, re-dissolved in methanol and centrifuged at $\sim 10{,}000 \times g$ for 20 min. The amount of BT released (%) at any time 't' was calculated using the formula:

$$\textit{Cumulative release}\ (\%) = \left(\frac{\textit{released amount of BT at time } t}{\textit{total amount of BT at time } 0}\right) \times 100. \quad (3)$$

Cytotoxicity evaluation of synthesized NVs by sulphorodamine B assay

Cytotoxicity of pure BT, PLA-1 NVs, PLA-2 NVs, BT-En-1 NVs and BT-En-2 NVs was evaluated using the sulfo-rhodamine B (SRB) method (Yadav et al. 2014a).

Results and discussion

Synthesis of PLA NVs

Betulin (BT) possesses strong anticancer activity. But, due to its poor aqueous solubility and low bio-accessibility, its use as a pharmaceutical is limited. Since BT is hydrophobic, PLA was used as a nanovector (NV) for its encapsulation. PLA NVs are mostly synthesized by single emulsion solvent evaporation method that requires stabilisers. The chemical stabilisers used for synthesis of PLA NVs may confer toxicity to them (Basarkar et al. 2007). These limitations have obliged us to look for alternate biogenic stabilisers.

We synthesized PLA NVs using PVA and leaf extracts (LEs) of *Lonicera japonica* as stabilisers. Synthesised NVs were evaluated and characterised for comparative encapsulation of betulin for the first time. PVA-mediated synthesis of PLA NVs named as PLA-1 NVs, and LEs-mediated synthesis of PLA NVs, named as PLA-2 NVs, were further used for encapsulation of BT. BT-encapsulated NVs were named as BT-En-1 and BT-En-2 NVs, respectively. The synthesized PLA-1 NVs, PLA-2 NVs, BT-En-1 NVs and BT-En-2 NVs were characterised by various techniques. PVA- and LEs-synthesized blank PLA NVs were prepared by a single emulsion method. Our studies have also documented the use of LEs for stabilizing PLA NVs (Yadav et al. 2011; Kumari et al. 2012). LEs contain many phytomolecules that act as stabilisers/emulsifiers (Kumar et al. 2010; Kumari et al. 2011; Kumari et al. 2012). Stabilisers play a vital role in stabilising emulsions formed during PLA NVs synthesis (Kumari et al. 2010b). Phytomolecules of LEs also showed good potential for stabilisation of emulsions formed during PLA NVs synthesis.

Spectroscopic characterisation of PLA-1 NVs, PLA-2 NVs, BT-En-1 NVs and BT-En-2 NVs

The initial confirmation of synthesis of PLA-1 NVs, PLA-2 NVs, BT-En-1 NVs and BT-En-2 NVs was conducted by UV–Vis spectroscopy. The PLA-1 NVs and PLA-2 NVs had a characteristic absorption peak at 229 nm (Fig. 1a, b), while that of pure BT was at 210 nm (Fig. 1a, b). Spectra of synthesized BT-En-1 and BT-En-2 NVs were different from pure BT (Fig. 1a, b), which indicated encapsulation of BT on PLA NVs. UV–Vis spectroscopy was used to confirm the initial synthesis of PLA NVs.

FTIR spectroscopy was used for the confirmation of loading of BT on PLA-1 and PLA-2 NVs. FTIR spectra of BT encapsulation in NVs had a peak intensity at 3384.8 cm^{-1} which appeared due to -OH group in the structure of BT. The band at 2995.7 cm^{-1} appeared to be due to asymmetrical $-CH_2$ stretching from the $-CH_2OH$. The peak at 1644.4 cm^{-1} may be assigned to –C=C– stretching and $-CH_2$ bending in the terminal methyl group. The band at 1044.1 cm^{-1} may be assigned to –C–O– stretching vibrations (Fig. 2a). The FTIR spectra of PLA-1 and PLA-2 NVs were different from the spectra of BT-En-1 NVs and BT-En-2 NVs (Supplementary Fig. 1). The characteristic peaks of BT were also found in FTIR spectra of BT-En-1 and BT-En-2 NVs. The appearance of similar IR bands of BT in BT-En-1 and BT-En-2 NVs spectrum confirmed the loading of BT in both types of BT-En-1 and BT-En-2 NVs (Fig. 2b). The FTIR spectra of

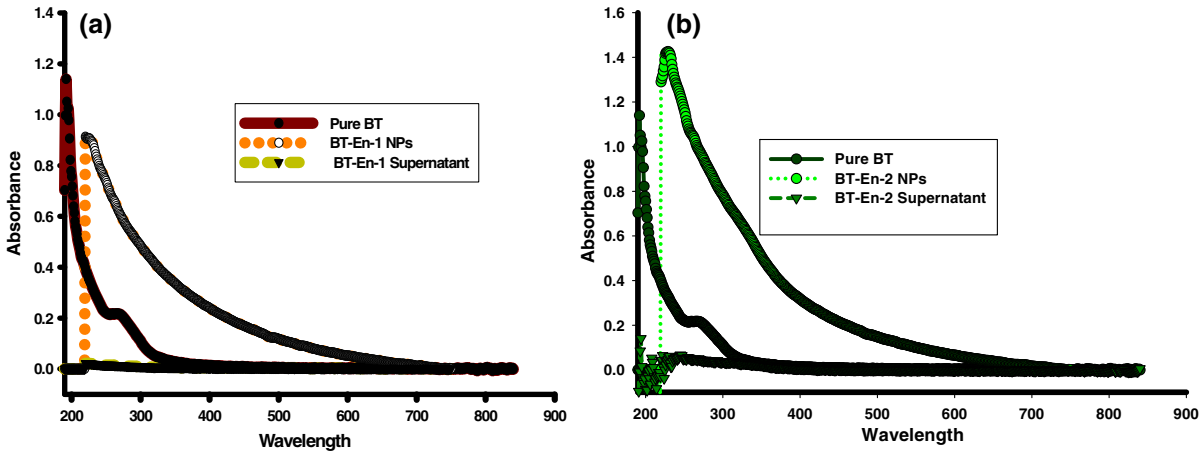

Fig. 1 UV–Vis spectral analysis of PLA NV and BT encapsulated NVs **a** UV–Vis spectra of the BT-En-1 NVs, pure BT and BT-En-1 NVs supernatant solution (obtained after separation of BT-En-1 NVs from mixture by centrifugation). **b** UV–Vis spectra of the BT-En-2 NVs, pure BT and BT-En-2 NVs supernatant solution (obtained after separation of BT-En-2 NVs from mixture by centrifugation)

PLA-1 NVs and PLA-2 NVs (Supplementary Fig. 1) provide evidence of BT loading in BT-En-1 NVs as well as in BT-En-2 NVs without any chemical interaction. FTIR peaks of BT obtained from BT-En-1 and BT-En-2 NVs spectra are in agreement with the FTIR spectra of BT reported earlier (Lugemwa 2012). FTIR spectroscopy also gives information about chemical molecules present on the surface of NVs as well as conformational changes (Honga et al. 2009; Luo et al. 2009). FTIR has also been used earlier for confirming the encapsulation of quercetin, quercitrin and curcumin in PLA NVs synthesized using PVA and turmeric extract (Kumari et al. 2010a, 2011; Kumar et al. 2014). FTIR spectroscopy of BT-En-1 and BT-En-2 NVs confirmed the loading of BT on PLA NVs.

Physical characterisation of PLA-1, PLA-2, BT-En-1 and BT-En-2 NVs

Size and morphology of PLA-1, PLA-2, BT-En-1, and BT-En-2 NVs were characterized by AFM, and TEM. AFM revealed that the PLA-1 NVs were spherical (Supplementary Fig. 2a). TEM revealed that yjr size of PLA-1 NVs was 145 ± 15 nm (Supplementary Fig. 2b) and BT-En-1 NVs was 138 ± 27 nm (Fig. 3Ab). AFM revealed that BT-En-1 NVs were smooth, and well dispersed (Fig. 3Aa). The size of PLA-2 NVs was 170 ± 15 nm (Supplementary Fig. 3b) compared to the 185 ± 15 nm of BT-En-2 NVs as revealed by TEM (Fig. 3Bb). The surface morphology of PLA-2 NVs (Supplementary Fig. 3a) and BT-En-2 NVs (Fig. 3Ba) were also smooth as observed by AFM.

The size and shape of NVs is a crucial parameter because it affects the cellular uptake mechanism and their ability to penetrate into tissues (Lu et al. 2009). PLA-1 and PLA-2 NVs were small and uniformly distributed. Different sized NVs accumulate in blood, liver, spleen, kidney, testis, thymus, heart, lung and brain (Kulkarni and Feng 2013). The uptake of NVs below 200 nm involves clathrin-coated pits (Nel et al. 2009). Small sized NVs (<100 nm) are retained in systemic circulation for longer duration. Morphological characterisation by TEM revealed that BT-En1 and BT-En-2 NVs were <200 nm.

The hydrodynamic diameter and zeta potential of synthesized PLA NVs were evaluated by DLS. PLA-1 and PLA-2 NVs were 250 ± 35 and 271 ± 20 nm, respectively (Supplementary Fig. 2d and Supplementary Fig. 3d) and BT-En-1 and BT-En-2 NVs were 276 ± 50 and 286 ± 42 nm (Fig. 3Ac, Bc), respectively. The greater hydrodynamic diameters of various NVs than those observed in the TEM images is reasonable because hydrodynamic diameters are larger than the core particle size measured by TEM (Ma et al. 2012).

Zeta potentials of PLA-1, PLA-2, BT-En-1 and BT-En-2 NVs were −23.5, −32.7, −26.8, and −32.0 mV

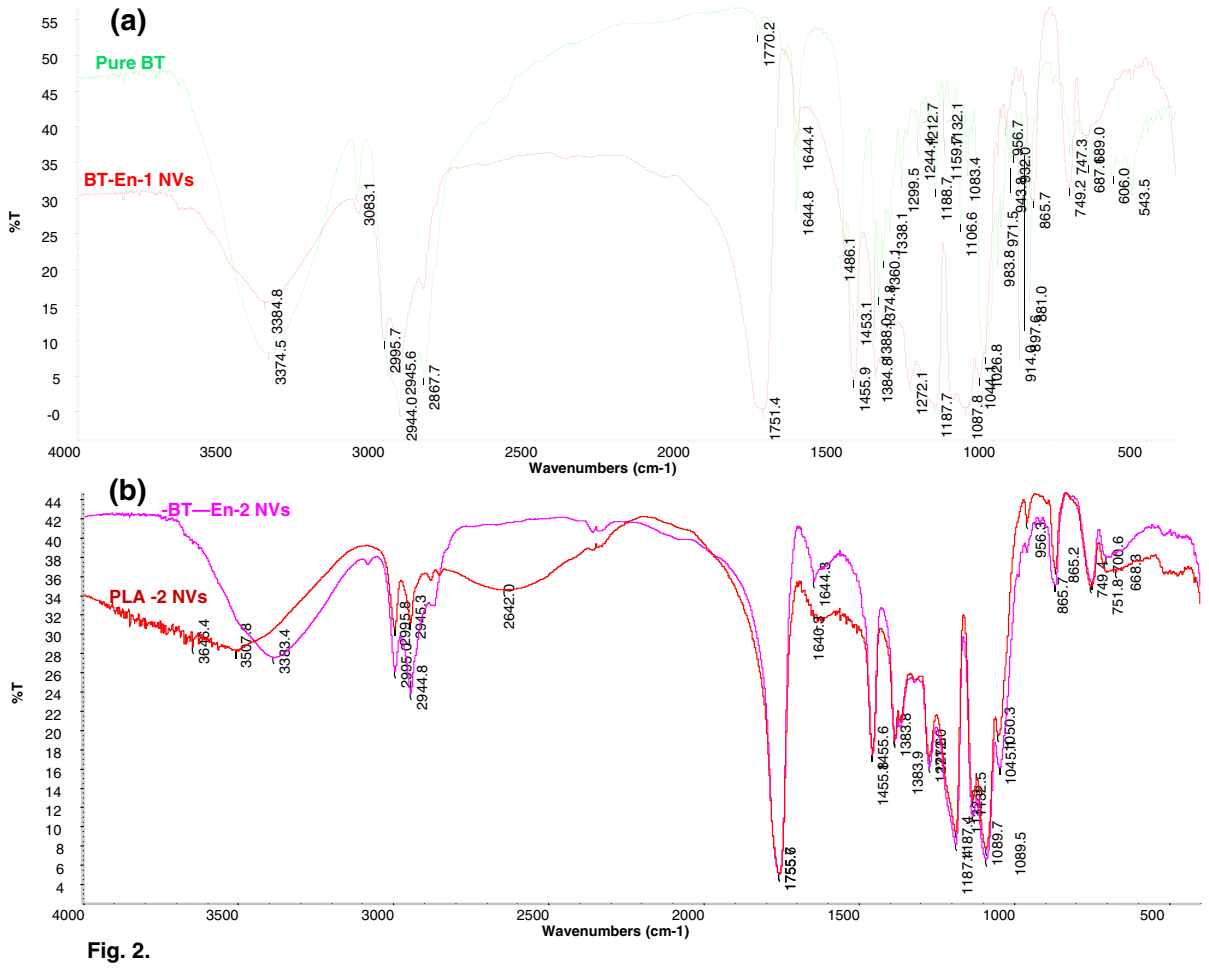

Fig. 2.

Fig. 2 FTIR spectra of pure BT, BT-En-1 NVs, PLA-2 NVs and BT-En-2 NVs. FTIR spectra was recorded on Thermo Nicolet 6700 FTIR spectroscopy (Thermo, USA). The appearance of characteristic bands of BT in IR spectrum of BT-En-1 NVs and BT-En-2 NVs indicated the successful loading of BT without any chemical interactions

respectively. Among these, the zeta potentials of PLA-2 and BT-En-2 NVs were more negative, indicating their better stability over the other NVs. Zeta potential measurements provide information about the surface charge of NVs which decide the fate of NVs inside the body.

Stability of PLA-1, PLA-2, BT-En-1 and BT-En-2 NVs

The stability studies of PLA-1, PLA-2, BT-En-1 and BT-En-2 NVs were carried out for 45 days at 37 °C using TEM and DLS to check the suitability for drug delivery (Supplementary Fig. 4). Size, shape and surface charge of PLA-1, PLA-2, BT-En-1 and BT-En-2 NVs were evaluated after 1, 5, 15, 30 and 45 days after synthesis. There was no change in the size and shape of PLA-1, PLA-2, BT-En-1 and BT-En-2 NVs during storage as revealed by TEM analysis (Fig. 4b–e). Also, no significant change was observed in the particle size of stored NVs compared with freshly prepared PLA-1, PLA-2, BT-En-1 and BT-En-2 NVs. The zeta potential was also measured to ascertain whether all type of synthesized PLA NVs had degraded or changed as a result of storage. The zeta potential of PLA-1 NVs decreased from −23.3 to −15.2 mV after 45 days (Fig. 4a). However, the zeta potential of PLA-2, BT-En-1, and BT-En-2 NVs changed only marginally during storage for 45 days (Fig. 4a). PLA-2 and BT-En-2 NVs showed a greater

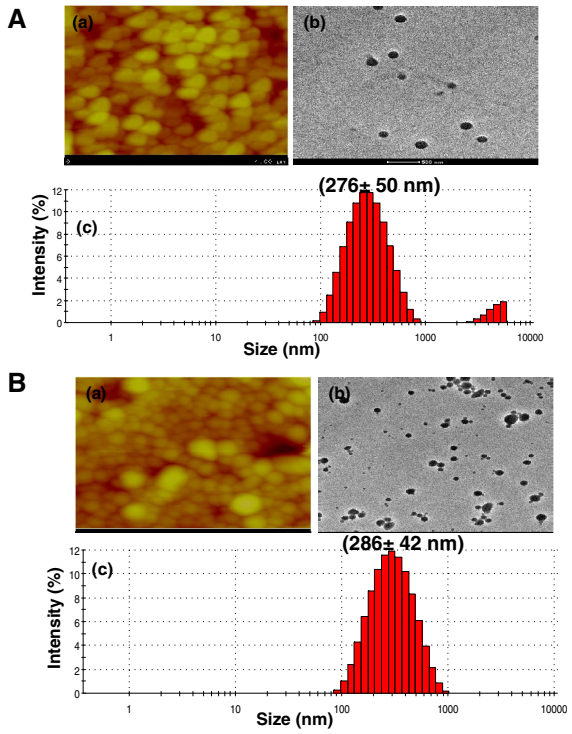

Fig. 3 **A** AFM image of BT-En-1 NVs (*a*), TEM image of BT-En-1 NVs (*b*) and DLS size of BT-En-1 NVs (*c*). **B** AFM image of BT-En-2 NVs (*a*), TEM image of BT-En-2 NVs (*b*) and DLS size of BT-En-2 NVs (*c*). AFM images of air dried NVs were captured on Nanscope-III in tapping mode. For TEM analysis a drop of NVs was placed on copper grid and negatively stained with 3 % ammonium molybdate. Images were recorded on Tecnai T20 Twin TEM at 200 kV. DLS measurements were carried in disposable cuvettes on Zeta sizer Nano ZS

zeta potential indicating good stability of LJLEs synthesized PLA NVs (Fig. 4a). Upon storage, the polydispersity index of PLA NVs increased from 0.143 to 0.273 indicating their existence in a non-aggregated form. TEM analysis results also supported the observations made by zeta potential measurements.

The stability of NVs is crucial towards the drug loading and drug delivery (Ranjan et al. 2013). PLA-2 and BT-En-2 NVs retained their stability at 37 °C after 45 days. Paclitaxel-loaded PLA NVs are also stable and show only a marginal increase in particle size on storage (Mishra and Trivedi 2013). Similarly, curcumin-loaded PLGA NV is stable for a long time (Ranjan et al. 2013). Storage temperature and duration also affect the size and surface charge of NVs (Nallamuthu et al. 2013). Thymoquinone-loaded PLGA NVs, however, retained their stability only for 15 min at elevated temperatures. Results of this present study indicate that LEs-synthesized PLA NVs could be ideal candidate for delivery of bioactive molecules at physiological temperature.

BT encapsulation in PLA-1 and PLA-2 NVs

To compare the performance of nanoformulations, encapsulation efficiency of BT on both types of PLA NVs synthesized using PVA and LEs were determined. To quantify BT, an HPLC method was developed. A BT standard curve was prepared (Supplementary Fig. 5b). The amount of BT was calculated on the basis of differences in the amount of BT in the initial formulation and supernatant obtained after separation of NVs. The physically encapsulated BT in PLA-1 and PLA-2 NVs was calculated with the help of the standard curve generated by HPLC (Supplementary Fig. 5a–c). BT encapsulation in PLA-1 NVs was 99 % (Supplementary Fig. 5a and Supplementary Fig. 5) while BT encapsulation in PLA-2 NVs was 100 % (Supplementary Fig. 5c). BT loading was 11.6 % and 12.5 % in BT-En-1 NVs and BT-En-2 NVs, respectively. Encapsulation efficiency and drug loading determines the performance of nanoformulations. Encapsulation efficiency of NVs depends on the synthesis method, type of NVs and interaction of bioactive molecules with NVs (Liviu et al. 2012). The BT loading in BT-En-1 and BT-En-2 NVs was similar to the loading of paclitaxel in NVs prepared with poly(L-lactic acid), poly(ε-caprolactone) and PLGA. Encapsulation efficiency of quercetin and curcumin on the LEs-synthesized PLA NVs is in a similar range (Kumar et al. 2014).

In vitro release of BT from BT-En-1 NVs and BT-En-2 NVs

In vitro release studies of BT-En-1 and BT-En-2 NVs were carried out in phosphate buffer/saline (PBS) which mimics physiological conditions. Released BT in PBS was quantified from the BT standard curve. An average of 1.4–7.5 % of BT was released within 0.5 h from BT-En-1 NVs and BT-En-2 NVs, respectively. The fast initial release might be attributed to the fraction of BT present on the surface of NVs. The release of BT from BT-En-1 NVs and BT-En-2 NVs showed a biphasic pattern. An average 19.8–29.6 % BT was released from BT-En-1 NVs and BT-En-2 NVs within 4 h (Fig. 5). The rapid initial release was

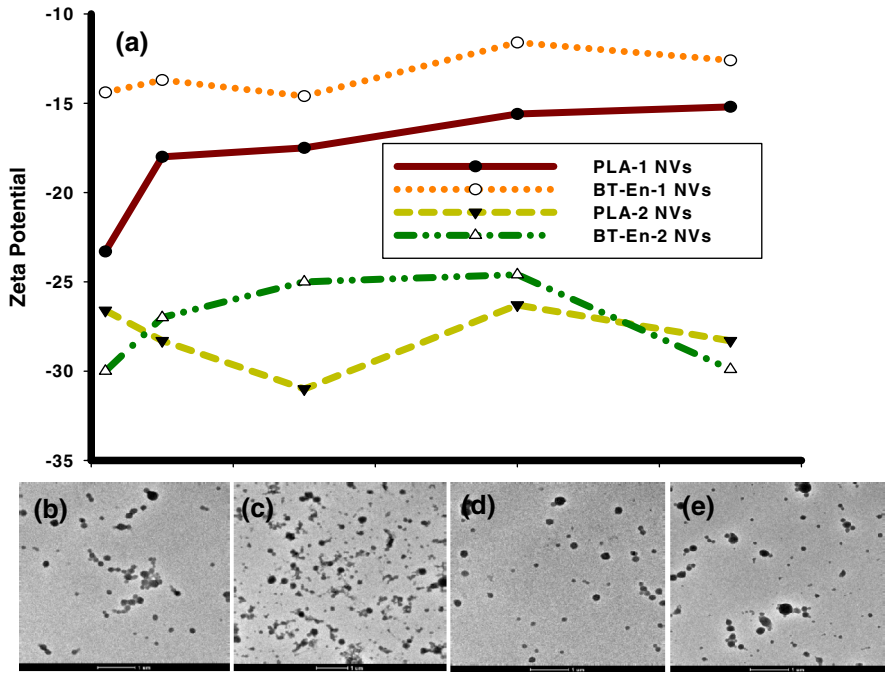

Fig. 4 **a** Physical stability of NVs was monitored by DLS and TEM plot of zeta potential values versus time in days **b** TEM image of PLA-1 NVs, **c** PLA-2 NVs, **d** BT-En-1 NVs and **e** BT-En-2 NVs. PLA-1 NVs, PLA-2 NVs, BT-En-1 and BT-En-2 NVs were kept at 37 °C for 45 days. Samples were collected at intervals for zeta potential measurements and TEM analysis

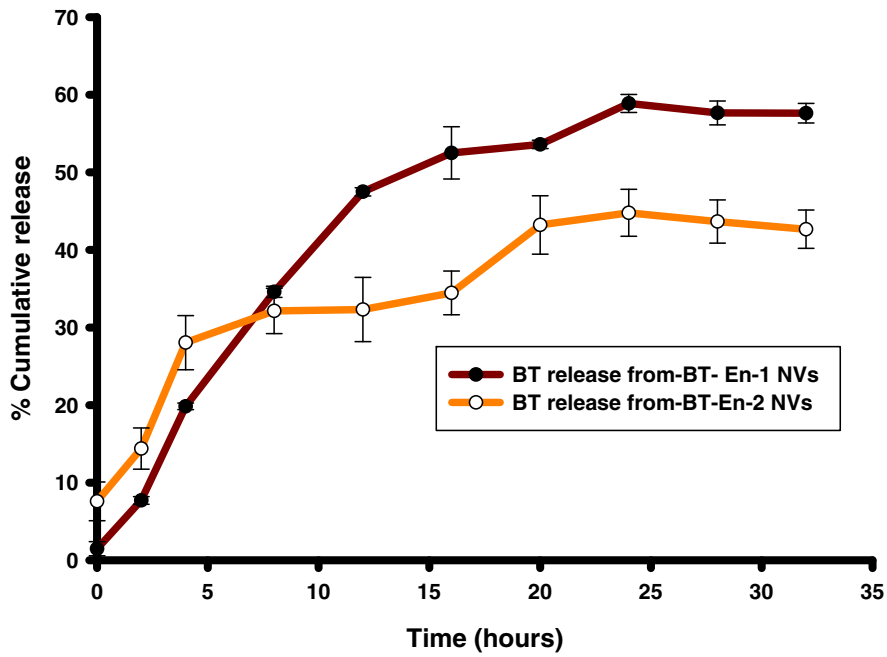

Fig. 5 Cumulative release (%) of BT from BT-En-1 and BT-En-2 NVs recorded by the HPLC. The release curve of BT was obtained by plotting percentage cumulative release of BT versus time

followed by a slow and sustained release. After 30 h, BT-En-1 NVs released 59 % BT. However, BT-En-2 NVs released 45 % BT in first 24 h.

In vitro release studies are important to document the successful use of nanomaterials in drug delivery systems. Release studies are also important to know the encapsulation or adsorption of bioactive molecules on NVs. Release rate of bioactive molecules from NVs is affected by the nature of drug, type and concentration of stabilisers. Release of bioactive molecules from

PLA NVs followed a diffusion and polymer degradation mechanism. BT showed slow and sustained release from both the formulations. BT showed a prolonged release rate from BT-En-2 NVs compared to BT-En-1 NVs. LEs did not affect the amount of BT present on the surface of NVs but possibly affected diffusion of BT from the PLA matrix. Bioactive molecules, such as quercetin, quercitrin, podophyllotoxin and curcumin, also show similar release patterns in physiological medium (Kumari et al. 2011, 2012; Yadav et al. 2011, 2014b; Kumar et al. 2014). The slow release of BT from PLA-2 NVs suggest they are good candidates for controlled release of bioactive molecules.

Cytotoxicity evaluation of pure BT, PLA-1, PLA-2, BT-En-1 and BT-En-2 NVs

In vitro cytotoxicity study of PLA-1, PLA-2, BT-En-1 and BT-En-2 NVs was conducted with SiHa cells using the SRB assay after 24, 48 and 72 h. PLA-1 and PLA-2 NVs were non-toxic against SiHa cells (Fig. 6a–c). The percent growth inhibition of SiHa cells was less than 50 % at all tested doses (5–50 µg/ml) of PLA-1 and PLA-2 NVs. At the highest tested dose, the percent growth inhibition was 48 ± 4.1 and 47.6 ± 0.9 for PLA-1 and PLA-2 NVs, respectively. These two formulations are thus as safe up to 50 µg/ml (Fig. 6a–c). The greater viability of SiHa cells in presence of PLA-1 and PLA-2 NVs suggests that these NVs are biocompatible for drug delivery.

BT-En-1 NVs showed 31 % growth inhibition at 50 µg/ml. BT-En-1 NVs gave growth inhibitions of 43.4 ± 2.1, 46.5 ± 1.9 and 50.6 ± 2.1 % at 10 µg/ml during 24, 48 and 72 h respectively. BT-En-2 NVs had a maximum 84 ± 1 % inhibition at 50 µg/ml while pure BT had a maximum 65.1 ± 4.5 % inhibition at 20 µg/ml. Hence, BT-En-2 NVs showed dose-dependent cytotoxicity against SiHa cells. Also, BT-En-2

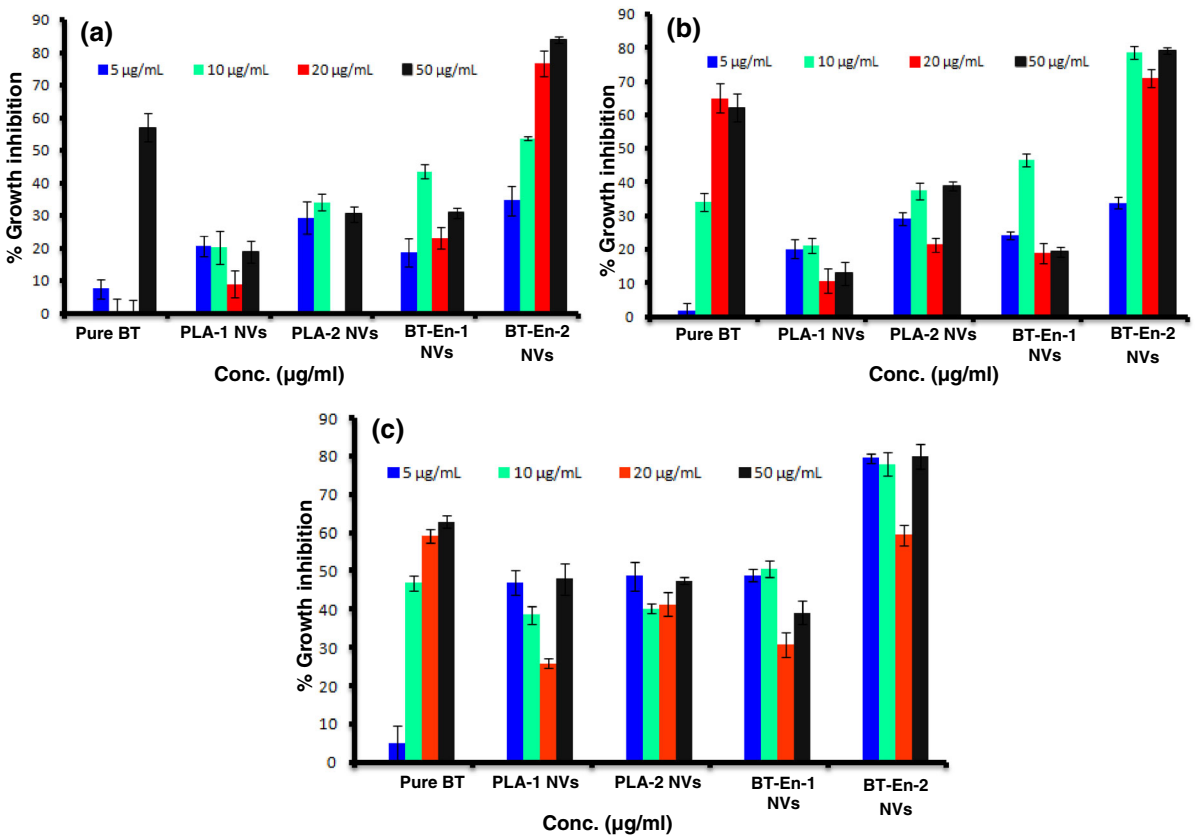

Fig. 6 In vitro cytotoxicity of PLA-1, PLA-2, BT-En-1 and BT-En-2 NVs. The cytotoxicity was tested against human cervical cancer cell line (SiHa) by SRB assay **a** 24 h, **b** 48 h and **c** 72 h

NVs had greater cytotoxicity than pure BT. Thus, encapsulation of BT in BT-En-2 NVs improves the efficacy of BT. The anticancer activity was attributed to BT as PLA-1 and PLA-2 NVs were non-toxic to SiHa cells.

For biomedical applications, evaluations of cytotoxicity and biocompatibility of the synthesized NVs are crucial (Kumari et al. 2010b; Yadav et al. 2014b). Plant-based stabilisers are safe for synthesis of PLA NVs. Therefore, cytotoxicity of PLA-1 NVs, PLA-2 NVs, BT-En-1 NVs and BT-En-2 NVs was assessed against SiHa cells using the SRB assay. PLA-1 NVs and PLA-2 NVs showed no cytotoxicity against SiHa cells. Turmeric extract-synthesized PLA NVs also are non-toxic against A549 cells (Kumari et al. 2012). BT-En-2 NVs showed greater activity than pure BT. Percentage growth inhibition values of BT-En-1 and BT-En-2 NVs did not match with the pure BT and indicated the slow release of BT. A similar slow release of temozolomide from PLGA NVs has been documented (Jain et al. 2014). Encapsulation of BT in BT-En-1 NVs and BT-En-2 NVs improves the solubility, bioavailability and sustained release. This could be overall responsible for improved anticancer activity of BT upon encapsulation. Different cytotoxicity behaviour of BT-En-1 NVs and BT-En-2 NVs against SiHa cells could be due to composition and type of stabilisers used. PLA-2 NVs synthesized with LEs were safe to SiHa cells. Hence, LEs-synthesized PLA NVs appeared to be a promising strategy for reducing harmful side effects and improving anticancer efficacy of BT.

Conclusions

Betulin (BT) loading on BT-En-1 NVs synthesized using PVA and on BT-En-2 NVs and using *Lonicera japonica* leaf extract (LEs) as stabiliser was 99.3 and 100 %, respectively. BT-En-1 NVs were smaller than BT-En-2 NVs. BT-En-2 PLA NVs gave a slow and controlled release. *In vitro* cytotoxicity study on SiHa cells revealed that BT-En-2 NVs were more toxic than BT-En-1 NVs. The good stability at physiological temperature, slow release characteristics and excellent biocompatibility of BT-En-2 NVs synthesized using LEs make it a potent candidate for loading of wide range of bioactive molecules and hence in pharmaceutical industry.

Acknowledgments Authors acknowledge Council of Scientific and Industrial Research, India for providing Senior Research Fellowship to RY. Authors are thankful to the Director, CSIR-IHBT, Palampur for continuous support and encouragement. Financial support in the form of research grant BSC-112 from CSIR is duly acknowledged. RY is also thankful to Academy of Scientific and Innovative Research, New Delhi.

Supporting information Supplementary Fig. 1—FTIR spectra of PLA -1 NPs and PLA-2 NPs.

Supplementary Fig. 2—Chracteriztion of PLA-1 NPs using AFM, TEM and DLS. AFM image of PLA-1 NPs (a) and TEM image of PLA-1 NPs (b). DLS size of PLA-1 NPs (c).

Supplementary Fig. 3—Chracterization of PLA-2 NPs using AFM, TEM and DLS. AFM image of PLA-2 NPs (a) and TEM image of PLA-2 NPs (b). DLS size of PLA-2 NPs (c).

Supplementary Fig. 4—Zeta potential and TEM image of PLA-1 NPs, PLA-2 NPs, BT-En-1 NPs and BT-En-2 NPs. PLA-1 NPs, PLA-2 NPs, BT-En-1 NPs and BT-En-2 NPs were stored at 37 °C for 45 days and TEM and zeta potential measurements were carried out to study their stability.

Supplementary Fig. 5—HPLC overlapped chromatograms of pure BT (a) and calibration curve of pure BT obtained using various concentration 1, 0.5, 0.25, 0.125, 0.0625 mg/ml) (b). The overlapped chromatogram of supernatants obtained after the seperation of various NPs through centrifugation (c).

References

Basarkar A, Devineni D, Palaniappan R, Singh J (2007) Preparation, characterization, cytotoxicity and transfection efficiency of poly(dl-lactide-co-glycolide) and poly(dl-lactic acid) cationic nanoparticles for controlled delivery of plasmid DNA. Int J Pharm 343:247–254

Gauthier C, Legault J, Lavoie S, Rondeau S, Tremblay S, Pichette A (2009) Synthesis and cytotoxicity of bidesmosidic betulin and betulinic acid saponins. J Nat Prod 72:72–81

Honga RY, Li JH, Zhanga SZ, Li HZ, Zheng Y, Ding JM, Wei DG (2009) Preparation and characterization of silica-coated Fe_3O_4 nanoparticles used as precursor of ferrofluids. Appl Surf Sci 255:3485–3492

Jager S, Laszczyk MN, Scheffler A (2008) A preliminary pharmacokinetic study of betulin, the main pentacyclic triterpene from extract of outer bark of birch. Molecules 13:3224–3235

Jain DS, Athawale RB, Bajaj AN, Shrikhande SS, Goel PN, Nikam Y, Gude RP (2014) Unraveling the cytotoxic potential of Temozolomide loaded into PLGA nanoparticles. DARU J Pharm Sci 22:1–9

Kulkarni SA, Feng SS (2013) Effects of particle size and surface modification on cellular uptake and biodistribution of polymeric nanoparticles for drug delivery. Pharm Res 30:2512–2522

Kumar V, Yadav SC, Yadav SK (2010) Syzygium cumini leaf and seed extract mediated biosynthesis of silver nanoparticles and their characterization. J Chem Technol Biotechnol 85:1301–1309

Kumar V, Kumari A, Kumar D, Yadav SK (2014) Biosurfactant stabilised anticancer biomolecule–loaded poly (D, L–lactide) nanoparticles. Colloid Surf B 117:505–511

Kumari A, Yadav SK, Pakade YB, Singh B, Yadav SC (2010a) Development of biodegradable nanoparticles for delivery of quercetin. Colloid Surf B 80:184–192

Kumari A, Yadav SK, Yadav SC (2010b) Biodegradabe nanoparticles based drug delivery systems. Colloid Surf B 75:1–18

Kumari A, Yadav SK, Pakade YB, Kumar V, Singh B, Chaudhary A, Yadav SC (2011) Nanoencapsulation and characterisation of *Albizia chinensis* isolated antioxidant quercitrin on PLA nanoparticles. Colloid Surf B 82:224–232

Kumari A, Kumar V, Yadav SK (2012) Plant extract synthesized PLA nanoparticles for controlled and sustained release of quercetin: a green approach. PLoS One 7:e41230

Liviu H, Floricuţa R, Diana C, Alina T, Carmen S (2012) Evaluation of betulin and betulinic acid content in birch bark from different forestry areas of western Carpathians. Not Bot Horti Agrobot 40:99–105

Lu F, Wu SH, Hung Y, Mou CY (2009) Size effect on cell uptake in well-suspended, uniform mesoporous silica nanoparticles. Small 5:1408–1413

Lugemwa FN (2012) Extraction of betulin, trimyristin, eugenol and carnosic acid using water-organic solvent mixtures. Molecules 17:9274–9282

Luo YB, Wang XL, Xu DY, Wang YZ (2009) Preparation and characterization of poly(lactic acid)-grafted TiO_2nanoparticles with improved dispersions. Appl Surf Sci 255: 6795–6801

Ma R, Levard C, Marinakos SM, Cheng Y, Liu J, Marc Michel F, Brown GE, Lowry GV (2012) Size-controlled dissolution of organic-coated silver nanoparticles. Environ Sci Technol 46:752–759

Mishra BJ, Trivedi P (2013) Formulation, stability and pharmacokinetic study of paclitaxel loaded poly (l-lactide) nanoparticles. Dig J Nanomater Biostruct 8:1829–1833

Mullauer FB, Kessler JH, Medema JP (2009) Betulin is a potent anti-tumor agent that is enhanced by cholesterol. PLoS One 4:e41230

Mustafaev M, Mustafaeva Z, Ergen E (2002) Novel betulin-containing polyelectrolyte conjugates. J Bioact Compat Polym 17:251–269

Nallamuthu I, Parthasarathi A, Khanum F (2013) Thymoquinone-loaded PLGA nanoparticles: antioxidant and antimicrobial properties. Int Curr Pharm J 2:202–207

Nel AE, Mädler L, Velegol D, Xia T, Hoek EMV, Ponisseril S, Klaessig F, Castranova V, Thompson M (2009) Understanding biophysicochemical interactions at the nano-bio interface. Nat Mater 8:543–557

Ranjan AP, Mukerjee A, Helson L, Vishwanatha JK (2013) Mitigating prolonged QT interval in cancer nanodrug development for accelerated clinical translation. J Nanobiotechnol 11:1–8

Soica C, Dehelean C, Danciu C, Wang HM, Wenz G, Rita A, Florina B, Mariana A (2012) Betulin complex in γ-cyclodextrin derivatives: properties and antineoplasic activities in in vitro and in vivo tumor models. Int J Mol Sci 13:14992–15011

Yadav SC, Kumari A, Yadav R (2011) Development of peptide and protein nanotherapeutics by nanoencapsulation and nanobioconjugation. Peptides 32:173–187

Yadav R, Kumar D, Kumari A, Yadav SK (2014a) Encapsulation of catechin and epicatechin on BSA NPs improved their stability and antioxidant potential. EXCLI J 13:331–346

Yadav R, Kumar D, Kumari A, Yadav SK (2014b) Encapsulation of podophyllotoxin and etoposide in biodegradable poly-D, L-lactide nanoparticles improved their anticancer activity. J Microencapsul 31:211–219